Excitation and ionization of a simple two-level system by a harmonic force

Excitation and ionization of a simple two-level system by a harmonic force

A Rokhlenko and J L Lebowitz[1]

Department of Mathematics, Rutgers University, Piscataway, NJ 08854-8019, USA

Abstract

A simple one-dimensional quantum system with two attractive δ-function potentials of strength q at $x \pm 1$ is subjected to a spatially asymmetric (as in the dipole interaction) harmonic forcing with frequency ω. The time evolution of the system, which has two discrete energy levels $-\omega_s < -\omega_a$ (depending on q) and a continuum spectrum, exhibits a rich dynamics including regimes where the rate of ionization becomes very small due to the 'inverse' Ramsauer effect in electron–atom collisions. The two-photon ionization with $\omega \approx \omega_s/2$ can be enhanced when $\omega_a = \omega_s/2$ though the one-photon ionization is not affected significantly by the location of excited level. When ω is very close to the one- or two-photon resonance the ionization rate can differ greatly from that given by the low order perturbation theory even for small forcing amplitude. This is caused in part by the fact that the dynamic Stark effect has a strong dependence on ω and may shift the resonance frequencies ω_s, ω_a up and down. When the ground state decays faster than the excited state and ω is not close to $\omega_s - \omega_a$, the excited level at late times becomes and remains more populated than the ground state. The occupations of the bound states oscillate with a frequency that can be quite low compared with ω, in particular in the case $\omega \approx \omega_a \approx \omega_s/2$, but it approaches ω when $\omega \gg \omega_s$.

Our analysis is based on the analytic structure of the wavefunction's Laplace transform in time. It considers one- and two-'photon' processes; the higher order multiphoton processes can also be treated by our computational scheme which goes beyond the low order perturbation theory.

PACS numbers: 32.80.Fb, 03.65.Ge, 32.60.+i, 31.15.Ar

1. Introduction

The excitation and ionization of atomic and molecular electronic states by external microwave and laser fields is well described by considering a quantum system interacting with a classical

[1] Also Department of Physics, Rutgers University, Piscataway, NJ 08854-8019, USA.

field. While there are many successful numerical and perturbative ways of analysing the behaviour of such systems [1] it is still useful, we believe, to study these phenomena using simplified model systems. This allows us to isolate the contribution of different features of such systems to experimental observations.

Following [2], we studied in [3–5] a one-dimensional model when a particle bound by a delta-function attractive potential is perturbed by a harmonic oscillation of the strength of the delta function. Our non-perturbative analysis showed that the ionization of this system exhibits a non-monotonic behaviour in the frequency and amplitude of perturbation similar to the dynamics of real atoms in electromagnetic fields. We also found that the decay of bound states has both exponential and power-law time dependence and that at resonances the decay is sometimes far from exponential. Similar results were obtained for other model systems in [1, 6] and they strongly suggest that the dynamics of ionization has a universal character.

In this work, we extend the analyses [3–5] and [2, 7] to systems having more than one bound state in order to study the interplay between inter-level transitions and ionization (transitions to the continuum) induced by a strong periodic forcing [8]. We are particularly interested in understanding how these transitions are affected by the level spacing for different strengths and frequencies of the external force including situations involving multiphoton processes (see [9]). For a detailed analysis, we want to get a reliable analytical solution of the problem at least for the one- and two-photon ionization. This requires us, as in [3–5], to go beyond the perturbation theory and use controllable approximations. As an interesting by-product of our modelling we demonstrate how the ionization dynamics might be affected by the Ramsauer resonance, a phenomenon, well known in atomic collisions [10, 11].

The model we study is a simple 1D 'molecule' with a Hamiltonian

$$H_0 = -\frac{\partial^2}{\partial x^2} + V_0(x), \qquad V_0(x) = -q[\delta(x+1) + \delta(x-1)], \qquad q > 0, \quad -\infty < x < \infty,$$
(1)

whose double well potential V_0 is perturbed by a time periodic potential $V_1(x) \sin \omega t$. The natural form of $V_1(x)$ is of course the dipole potential Ex, but for the reasons described above we shall instead consider a much simpler form of the same symmetry, namely

$$V_1(x) = qr[\delta(x-1) - \delta(x+1)].$$
(2)

In the absence of V_1 the system with Hamiltonian H_0 has two bound states when $q > 1$ but only one if $0 < q < 1$. It also has continuum states with energies k^2. Starting with the system in some initial bound state(s) at $t = 0$, the evolution of the wavefunction $\psi(x, t)$ is governed by the Schröedinger equation

$$i\frac{\partial}{\partial t}\psi(x, t) = [H_0 + V_1(x) \sin \omega t]\psi(x, t), \qquad t \geqslant 0.$$
(3)

We expect the present model to exhibit certain universal features of the ionization of real atoms (molecular dissociation) interacting with external electromagnetic fields, in which the internal structure of the system is important. A comparison of our analysis with the standard perturbation theory will be given in section 6.

We use the dimensionless units, $\hbar = 2m_e = a = 1$, where m_e is the particle mass and $2a$ is the space separation of our double well potential. The single parameter q in (1, 2) absorbs the strength of potential and this spacing; therefore the change of q can be attributed to one or both of these quantities.

2. The reference system

The continuum symmetric normalized eigenfunctions of the Hamiltonian H_0 are

$$\varphi_s(k, x) = \frac{1}{\sqrt{\pi}} \begin{cases} \dfrac{\cos(k + \phi_k)}{\cos(k)} \cos(kx), & \text{if} \quad |x| \leqslant 1, \\ \cos(k|x| + \phi_k), & \text{if} \quad |x| > 1, \end{cases} \tag{4}$$

where

$$\tan(k + \phi_k) = \tan k + q/k, \qquad k \geqslant 0.$$

The symmetric bound state, which exists for all $q > 0$, has the form

$$u_s(x) = \frac{\alpha}{\sqrt{2\gamma - q}} \begin{cases} e^{-\gamma} \dfrac{\cosh(\gamma x)}{\cosh(\gamma)}, & \text{if} \quad |x| \leqslant 1, \\ e^{-\gamma|x|}, & \text{if} \quad |x| > 1. \end{cases} \tag{5}$$

This is the ground state of the system with energy $-\omega_s = -\gamma^2$, where

$$\frac{2\gamma}{1 + e^{-2\gamma}} = q, \qquad \text{and} \qquad \alpha = \frac{\gamma}{\sqrt{1 + 2\gamma - q}}. \tag{6}$$

The antisymmetric wavefunctions of the continuum spectrum are of the form

$$\varphi_a(k, x) = \frac{1}{\sqrt{\pi}} \begin{cases} \dfrac{\sin(k + \mu_k)}{\sin(k)} \sin(kx), & \text{if} \quad |x| \leqslant 1, \\ \operatorname{sign}(x) \sin(k|x| + \mu_k), & \text{if} \quad |x| > 1, \end{cases} \tag{7}$$

where

$$\cot(k + \mu_k) = \cot(k) - q/k.$$

The system has, for $q > 1$, an excited antisymmetric bound state with energy $-\omega_a = -\lambda^2$ and the eigenfunction

$$u_a(x) = \frac{\beta}{\sqrt{q - 2\lambda}} \begin{cases} e^{-\lambda} \dfrac{\sinh(\lambda x)}{\sinh(\lambda)}, & \text{if} \quad |x| \leqslant 1, \\ \operatorname{sign}(x) e^{-\lambda|x|}, & \text{if} \quad |x| > 1, \end{cases} \tag{8}$$

where

$$\frac{2\lambda}{1 - e^{-2\lambda}} = q \qquad \text{and} \qquad \beta = \frac{\lambda}{\sqrt{1 + q - 2\lambda}}. \tag{9}$$

Equations (9) have no real solutions when $q < 1$. We shall take $q > 1$ from now on.

The ratio of the binding energies λ^2/γ^2 grows monotonically from zero to 1 when q grows from 1 to ∞. Thus, we can place the excited level anywhere between the ground state and the continuum by changing q. In particular when $q = 1 + \epsilon$, $(0 < \epsilon \ll 1)$ $\lambda \approx \epsilon$ and $\gamma \approx 0.64$ while if $q \approx 1.9638$ then $\gamma \approx 1.0924 \approx \sqrt{2}\lambda$, i.e. the excited bound state is equidistant from the ground state and the continuum, (compare (6) and (9)).

3. Time evolution of the forced system

We expand the solution of Schröedinger's equation (3) in terms of the eigenfunctions of H_0

$$\psi(x, t) = \theta_s(t) u_s(x) e^{i\omega_s t} + \theta_a(t) u_a(x) e^{i\omega_a t}$$
$$+ \int_0^\infty [\Theta_s(k, t) \varphi_s(k, x) + \Theta_a(k, t) \varphi_a(k, x)] e^{-ik^2 t} \, dk.$$

Assuming that the particle is initially bound,

$$\psi(x, 0) = \theta_s^0 u_s(x) + \theta_a^0 u_a(x), \qquad \left|\theta_s^0\right|^2 + \left|\theta_a^0\right|^2 = 1, \qquad \Theta_s(k, 0) = \Theta_a(k, 0) = 0, \tag{10}$$

and substituting $\psi(x, t)$ into equation (3), we obtain an expression for the expansion coefficients

$$\theta_s(t) = \theta_s^0 - 2\mathrm{i}\alpha \int_0^t \mathrm{e}^{-\mathrm{i}\gamma^2 t'} Y^+(t')\,\mathrm{d}t', \qquad \theta_a(t) = \theta_a^0 - 2\mathrm{i}\beta \int_0^t \mathrm{e}^{-\mathrm{i}\lambda^2 t'} Y^-(t')\,\mathrm{d}t', \tag{11}$$

$$\Theta_s(k, t) = -\frac{2\mathrm{i}\sqrt{q/\pi}}{\sqrt{1 + (\tan k + q/k)^2}} \int_0^t \mathrm{e}^{\mathrm{i}k^2 t'} Y^+(t')\,\mathrm{d}t',$$

$$\Theta_a(k, t) = -\frac{2\mathrm{i}\sqrt{q/\pi}}{\sqrt{1 + (\cot k - q/k)^2}} \int_0^t \mathrm{e}^{\mathrm{i}k^2 t'} Y^-(t')\,\mathrm{d}t'. \tag{12}$$

The functions

$$Y^\pm(t) = \sqrt{q}\, r \sin \omega t [\psi(1, t) \mp \psi(-1, t)]/2 \tag{13}$$

are to be found from two coupled integral equations

$$Y^-(t) = r \sin \omega t \left[\alpha \theta_s^0 \, \mathrm{e}^{\mathrm{i}\gamma^2 t} - 2\mathrm{i} \int_0^t K_s(t - t') Y^+(t')\,\mathrm{d}x' \right],$$

$$Y^+(t) = r \sin \omega t \left[\beta \theta_a^0 \, \mathrm{e}^{\mathrm{i}\lambda^2 t} - 2\mathrm{i} \int_0^t K_a(t - t') Y^-(t')\,\mathrm{d}t' \right], \tag{14}$$

whose kernels are

$$K_s(t) = \alpha^2 \, \mathrm{e}^{\mathrm{i}\gamma^2 t} + \frac{q}{\pi} \int_0^\infty \frac{\mathrm{e}^{-\mathrm{i}k^2 t}}{1 + (\tan k + q/k)^2}\,\mathrm{d}k,$$

$$K_a(t) = \beta^2 \, \mathrm{e}^{\mathrm{i}\lambda^2 t} + \frac{q}{\pi} \int_0^\infty \frac{\mathrm{e}^{-\mathrm{i}k^2 t}}{1 + (\cot k - q/k)^2}\,\mathrm{d}k. \tag{15}$$

Let $\tilde{F}(p)$ be the Laplace transform of a function $F(t)$, defined for Re $p > 0$ by

$$\tilde{F}(p) = \int_0^\infty \mathrm{e}^{-pt} F(t)\,\mathrm{d}t. \tag{16}$$

Then taking the Laplace transform of equations (14), (15) yields recurrence relations for $Y^\pm$ in the form

$$r^{-1}\tilde{Y}^-(p) = \frac{\omega\alpha\theta_s^0}{(p - \mathrm{i}\gamma^2)^2 + \omega^2} + \tilde{K}_s(p + \mathrm{i}\omega)\tilde{Y}^+(p + \mathrm{i}\omega) - \tilde{K}_s(p - \mathrm{i}\omega)\tilde{Y}^+(p - \mathrm{i}\omega), \tag{17a}$$

$$r^{-1}\tilde{Y}^+(p) = \frac{\omega\alpha\theta_a^0}{(p - \mathrm{i}\lambda^2)^2 + \omega^2} + \tilde{K}_a(p + \mathrm{i}\omega)\tilde{Y}^-(p + \mathrm{i}\omega) - \tilde{K}_a(p - \mathrm{i}\omega)\tilde{Y}^-(p - \mathrm{i}\omega). \tag{17b}$$

The functions $\tilde{K}(p)$ can be evaluated exactly (assuming Im $\sqrt{\mathrm{i}p} \geqslant 0$ when Re$(p) > 0$, see the appendix) to give

$$\tilde{K}_s(p) = \frac{\mathrm{i}q}{2[\sqrt{\mathrm{i}p}(\tan\sqrt{\mathrm{i}p} + \mathrm{i}) + q]}, \tag{18a}$$

$$\tilde{K}_a(p) = \frac{2\lambda^2(2\lambda - q)}{[1 - (q - 2\lambda)^2](p - \mathrm{i}\lambda^2)} - \frac{\mathrm{i}q}{2[\sqrt{\mathrm{i}p}(\cot\sqrt{\mathrm{i}p} - \mathrm{i}) - q]}. \tag{18b}$$
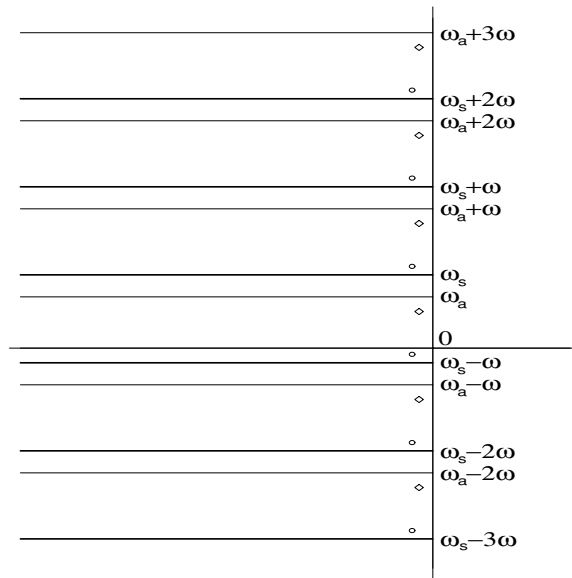
Figure 1. The p-plane with the cuts and poles which represents the analytic structure of $\tilde{Y}^{\pm}(p)$ for $\omega > \omega_s$. The circles indicate the poles produced by the ground state ($p = i\omega_s + \nu_s + ik\omega$) while the diamonds indicate the poles coming from the excited state ($p = i\omega_a + \nu_a + ik\omega$), k is an integer.

Note that on the imaginary p-axis both $\tilde{K}_{s/a}(p)$ in (18) are purely imaginary when $\mathrm{Im}(p) > 0$ and their real parts are positive when $\mathrm{Im}(p) < 0$.

Using the inverse Laplace transformation with $c > 0$ gives (11) in the form

$$
\begin{aligned}
\theta_s(t) &= \theta_s^0 - \frac{\alpha}{\pi} \int_{c-i\infty}^{c+i\infty} \frac{e^{pt}}{p} \tilde{Y}^+(p + i\gamma^2) \, dp, \\
\theta_a(t) &= \theta_a^0 - \frac{\beta}{\pi} \int_{c-i\infty}^{c+i\infty} \frac{e^{pt}}{p} \tilde{Y}^-(p + i\lambda^2) \, dp.
\end{aligned}
\tag{19}
$$

The integrations in (19) have to take into account the structure of $\tilde{Y}^{\pm}(p)$ which are analytic in the right half p-plane and singular in the left one, see figure 1. In particular, the location of poles gives the decay exponents of $\theta_s(t)$ and $\theta_a(t)$ as well as the energy shift of the perturbed bound levels—the dynamic Stark effect [11, 12]. Our problem now is to solve the recurrence (17) and after this evaluate the integrals in (19).

3.1. Notation

Before going on to describe our approximate solution of (17) and computation in (19), we introduce some notation which will be useful later. We define the following functions of p and ω

$$
\begin{aligned}
S_n &= \frac{\omega\alpha\theta_s^0}{(p + in\omega - i\gamma^2)^2 + \omega^2}, &\qquad A_n &= \frac{\omega\beta\theta_a^0}{(p + in\omega - i\lambda^2)^2 + \omega^2}, \\
s_n &= \tilde{K}_s(p + in\omega), &\qquad a_n &= \tilde{K}_a(p + in\omega), &\qquad \tilde{Y}_n^{\pm} &= \tilde{Y}^{\pm}(p + i\omega n); \\
b_k^- &= S_k + r(s_{k+1}A_{k+1} - s_{k-1}A_{k-1}), &\qquad c_k^- &= 1 + r^2 a_k(s_{k+1} + s_{k-1}), \\
b_k^+ &= A_k + r(a_{k+1}S_{k+1} - a_{k-1}S_{k-1}), &\qquad c_k^+ &= 1 + r^2 s_k(a_{k+1} + a_{k-1}),
\end{aligned}
$$

$$f_n^- = \frac{a_{2n}}{c_{2n}^-} s_{2n-1}, \qquad g_n^- = \frac{a_{2n}}{c_{2n}^-} s_{2n+1}, \qquad f_n^+ = \frac{s_{2n}}{c_{2n}^+} a_{2n-1},$$

$$g_n^+ = \frac{s_{2n}}{c_{2n}^+} a_{2n+1}, \qquad k, n \in Z.$$

$$(20)$$

By eliminating $\tilde{Y}^-$ and $\tilde{Y}^+$ from (17a) and (17b) respectively equations (17) can be rewritten in the form of two quasi-independent recurrence relations on a periodic grid with $-\omega \leqslant \mathrm{Im}\, p < \omega$

$$c_k^- \tilde{Y}_k^- = r b_k^- + r^2 \left(s_{k+1} a_{k+2} \tilde{Y}_{k+2}^- + s_{k-1} a_{k-2} \tilde{Y}_{k-2}^- \right),$$
$$c_k^+ \tilde{Y}_k^+ = r b_k^+ + r^2 \left(a_{k+1} s_{k+2} \tilde{Y}_{k+2}^+ + a_{k-1} s_{k-2} \tilde{Y}_{k-2}^+ \right).$$

$$(21)$$

4. Approximate solutions

The problem of solving the recurrence relations (21) can be done in principle with any precision using continuous fractions which represent the solution by a convergent procedure for arbitrary r and ω [3–5]. In practical terms one can obtain a good approximate solution by truncating (21), i.e. by assuming $\tilde{Y}_k \equiv 0$ for all $k > N$ or $k < -M$ with some positive N, M depending on ω and r. Equations (21) then get replaced by a finite set of linear algebraic equations whose solution will contain products of the functions $r s_k, r a_k$, see (21). The contributions from terms with large $|k|$ decay rapidly due to the increasing arguments of s_k, a_k and powers of r when r is not too large. If $|k|$ is not large and $\omega_s + k\omega, \omega_a + k\omega$ are not close to 0 then the coefficients s_k, a_k are of order of 1. Near the singularities (see (18) and (20)), i.e. $p + \mathrm{i}k\omega = \mathrm{i}\omega_s$ or $p + \mathrm{i}k\omega = \mathrm{i}\omega_a$, the functions s_k, a_k become large, but in the strip $0 \leqslant \mathrm{Im}\, p < \omega$ this can happen only for $0 \leqslant k \leqslant \omega_s/\omega$. Therefore for small r one can truncate (21) at some $M = N > \omega_s/\omega$ and evaluate $\tilde{Y}(p)$ up to $O(r^{2N})$. Thus all the important terms are included in the computation, namely up to N-'photon' processes. In the case when ω_s/ω is large it would be more effective for computation to take $M < N$. (Successive truncations give a convergent procedure for all r, but because the products of $r s_k, r a_k$ will go through their maxima, when the number of terms in these products grow, a careful evaluation of N, M is needed for large r).

Choosing $N = 3$ allows us to get the ionization rates and Stark shifts up to order r^6 when two 'photons' are sufficient for the ionization, i.e. when

$$2\omega > \omega_s + \text{dynamic Stark shift.} \tag{22}$$

For these values of ω the terms which represent three and more photons do not give resonant contributions. Solving the algebraic system, which comes from the truncated recurrence (21), we obtain $\tilde{Y}^\pm(p)$ in the form of two fractions whose denominators have only even powers of r; for details see the appendix. Zeros of these denominators represent the poles of $\tilde{Y}$ and resonances of $\tilde{\psi}$. The real and imaginary parts of coordinates of these poles correspond respectively to the decay exponents of the bound states and the dynamic Stark shifts.

Note that in contrast with the standard perturbation techniques, our approximate analysis never gives divergences at the resonances. Therefore, the dynamics can be studied for all frequencies $\omega > \omega_s/2$ without exceptions. In addition, we have the flexibility to evaluate terms of different importance to different order in r. The dynamical Stark effect comes naturally from the computations even in the lowest level of truncation of (21). It appears that one can have about 1% precision in the decay exponents by dropping terms of order

r^6 for $r \leqslant 0.5$. For computing prefactors we may neglect even terms of order r^4, giving an error of about 6% in the details of the $\theta(t)$ oscillations (but this significantly simplifies calculations because the decay exponents can be found from (21) without actual iterations there). Comparison with the first-order perturbation theory will be given in section 6.

The poles in figure 1 are shifted into the left half plane from their unperturbed ($r \to 0$) locations on the imaginary axis by the small (usually) complex numbers ν_s, ν_a. The initial poles at $p = i\omega_s$ and $p = i\omega_a$ represent the ground and excited states respectively. These are shifted to $i\omega_s + \nu_s$, $i\omega_a + \nu_a$ and are repeated periodically in $i\omega$. They are evaluated in the process of solving (21) as functions of ω and r. Thus, the $\sin \omega t$ perturbation creates from two original poles of the Laplace transform of the unperturbed wavefunction two infinite sets of resonances of $\tilde{\psi}(x, p)$ in the p-plane.

Computation of ν_s, ν_a, carried out in the appendix, yields two independent transcendental equations for the location of the poles of $\tilde{Y}^{\pm}$ respectively,

$$\nu_a = -r^2\beta^2(s_1 + s_{-1}) + r^4\beta^2\left[a_2 s_1^2 + a_{-2} s_{-1}^2 - i f_a(s_1 + s_{-1})^2\right], \qquad \text{at} \quad p = i\omega_a + \nu_a,$$
$$\nu_s = -r^2\alpha^2(a_1 + a_{-1}) + r^4\alpha^2\left[s_2 a_1^2 + s_{-2} a_{-1}^2 - i f_s(a_1 + a_{-1})^2\right], \qquad \text{at} \quad p = i\omega_s + \nu_s,$$

$$(23)$$

where a_n, s_n are defined in (20) and

$$f_s = \frac{1 + (q - 2\gamma)(1 + 2\gamma - 2q)}{4(1 + 2\gamma - q)^2}, \qquad f_a = \frac{1 + (q - 2\lambda)(1 + 2\lambda - 2q)}{4(1 + 2\lambda - q)^2}.$$

Equations (23), in which terms of order r^6 are neglected, can be easily solved by iterations. The properties of $\tilde{K}_{s/a}(p)$ imply (see (18) and (23)) that if the ground state can be ionized by a single photon, i.e. $\omega > \omega_s$, then both ν_a and ν_s have real and imaginary parts of order r^2. When ω decreases and $\omega_a < \omega < \omega_s$ the real component of ν_s becomes of order r^4 and for $\omega < \omega_a$ the same happens with $\text{Re}(\nu_a)$ too. The real parts are negative and they determine the decay exponents for the envelopes of $\theta_s(t)$ and $\theta_a(t)$ respectively during the intermediate stage of their evolution. $\text{Im }\nu_s$ and $\text{Im }\nu_a$, which are always of order r^2, give the dynamic Stark shift of the energy levels. The transition from one- to two-photon regimes is also affected by the Stark effect which is not indicated here for simplicity because the shifts ν_s, ν_a depend on ω and r.

Besides poles the functions $\tilde{Y}^{\pm}$ also inherit from (18) an infinite set of cuts, see figure 1. This suggests evaluating the amplitudes $\theta_{s/a}(t)$ in (19) by deforming the path of integration into contours around poles and cuts, like we did in [3–5]. For $r < 0.6$ we may restrict our analysis to taking into consideration only the poles of $\tilde{Y}(p)$ when computing (19). The integrals around the cuts give zero contributions to $\theta(t)$ at $t = 0$ and are of order r^3. It was proven rigorously in [3, 4], for the Hamiltonian with one attractive δ-function, that these terms determine in one dimension the $t^{-3/2}$ tail of $\theta(t)$ when $t \to \infty$ which is similar to the decay of bound states via tunnel effect at very large t [6]. Only for $r^2 t \gg 1$ (or $r^4 t \gg 1$ in the two-'photon' situation) the integrals around cuts become important (note that when r is large their contributions cannot be separated from the residues in (19)). Keeping in mind that for $n \sim 1$, $\omega \sim 1$ and far from resonances s_n, a_n are of order 1 too, we compare two quantities $\exp(-r^{2n}t)$ and $r^3 t^{-3/2}$ when t is large. The first term models the exponential decay which comes from poles for the n-photon processes and the second one describes qualitatively the contribution from the cuts in figure 1. A simple estimate shows that when t is such that these terms become equal for $r = 0.1, 0.2, 0.5$ their values are 1.2×10^{-8}, 1.3×10^{-6}, 8.4×10^{-4} respectively if $n = 1$ and 7.6×10^{-12}, 6.3×10^{-9}, 6.5×10^{-5} if $n = 2$. Thus, for moderate r using only the residues of integrands in (19) is a good approximation if t is not very large.

5. Results

To carry out the integration in (19) we compute (see the appendix) the residues of integrands there at 14 points $p = i\lambda^2 \pm in\omega + v_a$, $p = i\gamma^2 \pm in\omega + v_s$ with $n = 0, 1, 2, 3$. The result of this computation yields analytic expressions (A.7) for the time evolution of projections of the wavefunction $\psi(x, t)$ on the bound states which are good approximations for all $\omega > \omega_s/2$ and $r < 0.7$. A simplified form of (A.7) for r very small, ω not close to resonances, and $|\Delta - \omega| \gg r$ is

$$
\begin{aligned}
\theta_s(t) &= T_s\,\mathrm{e}^{v_s t}\left(1 - \mathrm{i}r^2\alpha^2\frac{a_1\,\mathrm{e}^{2\mathrm{i}\omega t} + a_{-1}\,\mathrm{e}^{-2\mathrm{i}\omega t}}{2\omega}\right) + 2\mathrm{i}r\alpha\beta T_a\frac{\omega\cos\omega t + \mathrm{i}\Delta\sin\omega t}{\omega^2 - \Delta_a^2}\,\mathrm{e}^{-\mathrm{i}\Delta_a t}, \\
\theta_a(t) &= T_a\,\mathrm{e}^{v_a t}\left(1 - \mathrm{i}r^2\beta^2\frac{s_1\,\mathrm{e}^{2\mathrm{i}\omega t} + s_{-1}\,\mathrm{e}^{-2\mathrm{i}\omega t}}{2\omega}\right) + 2\mathrm{i}r\alpha\beta T_s\frac{\omega\cos\omega t - \mathrm{i}\Delta\sin\omega t}{\omega^2 - \Delta_s^2}\,\mathrm{e}^{\mathrm{i}\Delta_s t},
\end{aligned}
\tag{24}
$$

where α, β are defined in (6), (9), $\Delta = \omega_s - \omega_a$ and,

$$
T_a \equiv \theta_a^0 - \frac{2\mathrm{i}r\alpha\beta\omega\theta_s^0}{\omega^2 - \Delta_a^2}, \qquad T_s \equiv \theta_s^0 - \frac{2\mathrm{i}r\alpha\beta\omega\theta_a^0}{\omega^2 - \Delta_s^2}, \qquad \Delta_s = \Delta - \mathrm{i}v_s, \quad \Delta_a = \Delta + \mathrm{i}v_a.
\tag{25}
$$

We dropped here terms of order r^3 which decay as linear combinations of $\mathrm{e}^{v_a t}$ and $\mathrm{e}^{v_s t}$. In (24) a_1, a_{-1} are taken at $i\omega_s + v_s$ while s_1, s_{-1} at $i\omega_a + v_a$.

Equations (A.7) and sometimes (24, 25) together with (23) are used for all our plots below where we consider three locations of the excited level corresponding to three different values of q: (i) $q = 1.963\,83$, ($\omega_a = \omega_s/2$), i.e. the excited level is equidistant from the ground one and continuum, (ii) $q = 1.5046$, ($\omega_a = \omega_s/4$), the excited state is closer to continuum and (iii) $q = 2.701\,79$, ($\omega_a = 3\omega_s/4$) where it is closer to the ground level.

5.1. Decay exponents and Stark effect

Decay exponents of the bound states are twice the real parts of v_s, v_a, while the dynamic Stark shifts of the energy levels ω_s, ω_a are determined by $\mathrm{Im}\,v_s$ and $\mathrm{Im}\,v_a$ respectively. Far from resonances one can drop terms $O(r^4)$, i.e. neglect v_s, v_a on the right-hand sides of (23), and when the one-photon processes are permitted equations (18), (23) yield

$$
\begin{aligned}
\mathrm{Re}\,v_s &\approx -\frac{r^2\alpha^2 q}{2\sqrt{\omega - \omega_s}[1 + (\cot\sqrt{\omega - \omega_s} - q/\sqrt{\omega - \gamma^2})^2]} & \text{for} \quad \omega > \omega_s, \\
\mathrm{Re}\,v_a &\approx -\frac{r^2\beta^2 q}{2\sqrt{\omega - \omega_a}[1 + (\tan\sqrt{\omega - \omega_a} + q/\sqrt{\omega - \lambda^2})^2]} & \text{for} \quad \omega > \omega_a.
\end{aligned}
\tag{26}
$$

Closer to the resonances we have to solve equation (23) iteratively and such an explicit presentation of v_s, v_a is impossible. In figures 2–4 are plotted the decay parameters for the cases (i), (ii) and (iii) when $r = 0.1$.

We can see in (26) and in figures 2–4 that at special frequencies

$$
\omega = \omega_s + l^2\pi^2, \qquad l = 1, 2, \ldots
\tag{27}
$$

$\mathrm{Re}\,v_s \approx 0$ to the lowest order in r^2. Thus asymptotically $|\theta_s(t)| \gg |\theta_a(t)|$. If

$$
\omega = \omega_a + (l - 1/2)^2\pi^2
\tag{28}
$$

the situation is the opposite: $\mathrm{Re}(v_a) \approx 0$ and when $t\,\mathrm{Re}(v_s) \gg 1$ we have $|\theta_a(t)| \gg |\theta_s(t)|$ even for $\theta_a(0) = 0$ like in figures 2 and 5. The slowly decaying odd state 'feeds' the ground
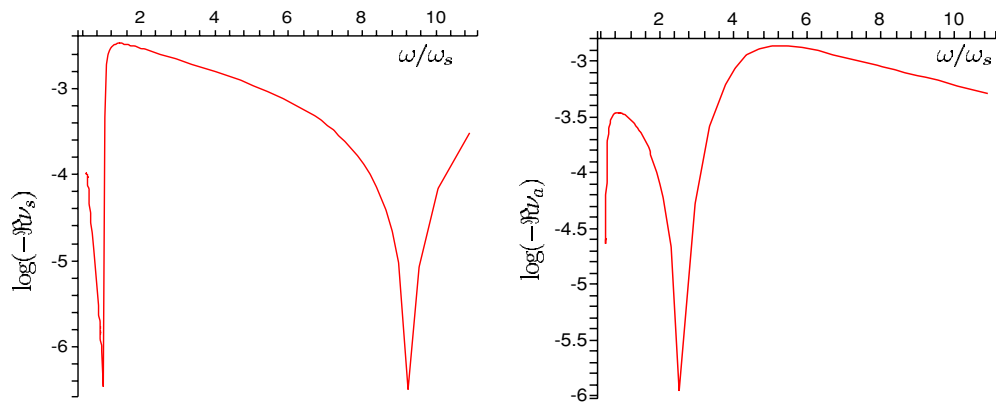
Figure 2. Plots of $\log(-\mathrm{Re}\,\nu_s)$ and $\log(-\mathrm{Re}\,\nu_a)$ when $\omega_a = 0.5\omega_s$ and $r = 0.1$.
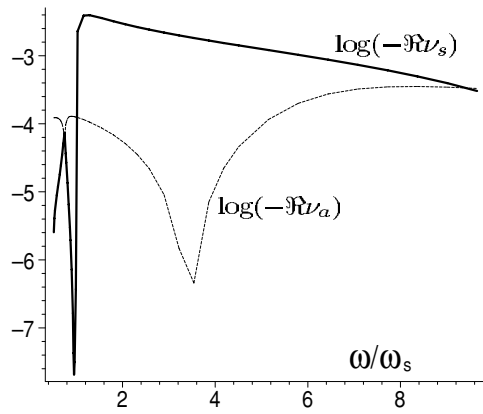
Figure 3. Plots of $\log(-\mathrm{Re}\,\nu)$ when $\omega_a = 0.25\omega_s$.
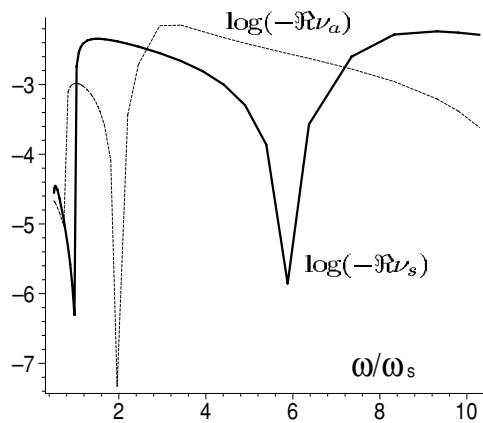
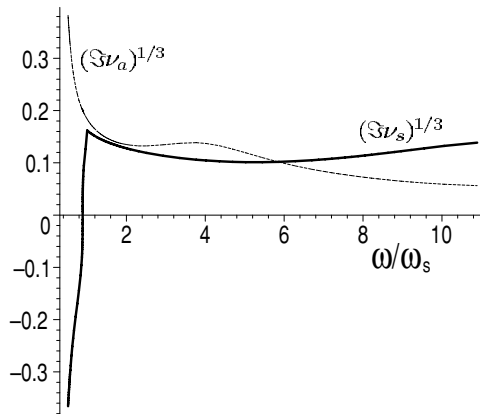**Figure 4.** Plots of $\log(-\mathrm{Re}\,\nu)$ for $\omega_a = 0.75\omega_s$.

Figure 5. Plots of $(\mathrm{Im}\,\nu_s)^{1/3}$ and $(\mathrm{Im}\,\nu_a)^{1/3}$ when $\omega_a = 0.5\omega_s$ and $r = 0.1$.

state. In terms of the perturbation theory when ω satisfies (27) or (28) vanish the matrix elements

$$\langle u_s|V_1|\phi_a(k)\rangle = \frac{2rq\alpha \sin\omega t}{\sqrt{\pi q[1 + (\tan k + q/k)^2]}}, \qquad \langle u_a|V_1|\phi_s(k)\rangle = \frac{2rq\beta \sin\omega t}{\sqrt{\pi q[1 + (\cot k - q/k)^2]}}$$

and thus transitions to the continuum become forbidden. For $k = \left(l - \frac{1}{2}\right)\pi$ and $k = l\pi$ the eigenfunction (4) or (7) respectively of the continuum spectrum is the same as that of the free particle, i.e. $\sim\pi^{-1/2}\cos kx$ or $\pi^{-1/2}\sin kx$, which corresponds to the Ramsauer's effect [10, 11] when an external particle (an electron) does not interact (scatter) with the potential field in H_0. When the frequency of the perturbation satisfies (27) or (28) the electron being kicked out of the bound state would get exactly such a momentum k which makes it 'free' of interaction. Correspondingly the bound state too cannot interact with the field of this frequency: the transition is forbidden. This is true only in the lowest order in r, when the transitions into the continuum spectrum are caused by a single photon whose frequency satisfies (27) or (28). If $\omega_a < \omega < \omega_s$, i.e. the ionization of the ground state requires more than one photon, (28) does not hold, but this effect is still possible for the excited state (whose decay otherwise is governed by $\nu_a \sim r^2$) and both decay exponents, see (23), can be of order r^4. If $a_{-2}(\mathrm{i}\lambda^2)$ or $s_{-2}(\mathrm{i}\gamma^2)$ are imaginary (small ω) the decay will be even slower, but we study here only the situation when the two-photon process is possible, i.e. $\omega > \omega_s/2$.

It is also seen in figures 2–4 that in the one-photon processes the following holds: (1) the maximum values of the decay exponents do not depend strongly on the location of the excited state between the ground one and the continuum, (2) the Ramsauer minima of ν slow down the decay very sharply (and there the contributions from cuts of $\tilde{Y}$ might be dominant), (3) the decay exponents in general decrease when $\omega > 1$ increases thus manifesting the behaviour of the energy level density in our 1D problem [10–12].

The dynamic Stark effect can also be obtained from the solutions of (23). Its dependence on ω/ω_s is shown in figures 5 and 6 for the cases (i) and (ii). Typically the shifts of the ground and excited energy levels are positive, i.e. they move the levels deeper from their unperturbed locations ω_s, ω_a thus 'resisting' the ionization. When $\omega \sim \omega_s/2$ the levels shift in the opposite directions (see figure 6): one them goes up but the other becomes slightly more shallow. This makes the transition between them less probable. This effect might reflect the fact that trajectories of the solutions of equation (23) 'repulse' each other: the bound particle after absorbing a photon in the ground state 'does not want' to get the energy $\Delta + \mathrm{Im}(\nu_s - \nu_a)$.
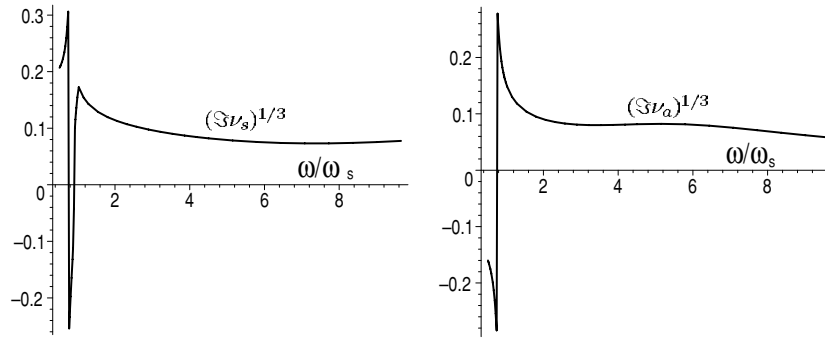
Figure 6. Plots of $(\mathrm{Im}\,\nu_s)^{1/3}$, $(\mathrm{Im}\,\nu_a)^{1/3}$ when $\omega_a = 0.25\omega_s$ and $r = 0.1$.
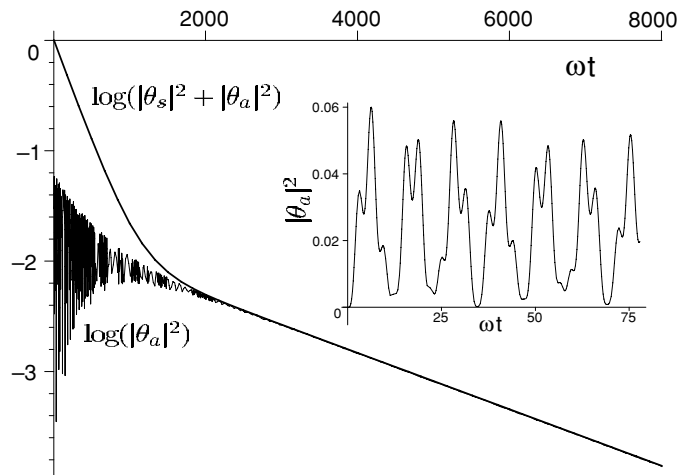

Figure 7. Plots of $\log(|\theta_a(t)|^2)$ and $\log(|\theta_s|^2 + |\theta_a|^2)$. Graph of $|\theta_a(t)|^2$ for short times is shown in the inset.

5.2. Dynamics of energy level population

We consider the time evolution of the survival probabilities for the initial condition $\theta_s(0) = 1$, $\theta_a(0) = 0$. The inter-level transitions partially populate the excited state and both levels decay initially with their own rates which are generally different. One can expect that if, (1) the decay exponent of the excited level is smaller than that of the ground state and (2) the inter-level transitions are not very effective, then the population of the excited state $|\theta_a|^2$ after some time becomes larger than $|\theta_s|^2$.

In figure 7, we plot the survival probability in a one-photon ionization process for the case $r = 0.1$, $\omega_a = \omega_s/2$ and $\omega = 1.3$.

During early times the excited state's population is very low (see the inset), it oscillates and decays much slower than the ground state and the ionization goes mainly directly from the ground level. The decay exponents are $\nu_s \approx -2.8 \times 10^{-3}$, $\nu_a \approx -3.8 \times 10^{-4}$. Figure 7 shows that after about 99% of the initial population is ionized what is left is mostly in the excited level from where it continues to decay. We conclude that the presence of the continuum spectrum allows the inversion of population in the dynamic regime. Excited states of real atoms have typically [10, 13] a lifetime T for spontaneous decay of order 10^{-8} s. Thus, if we map
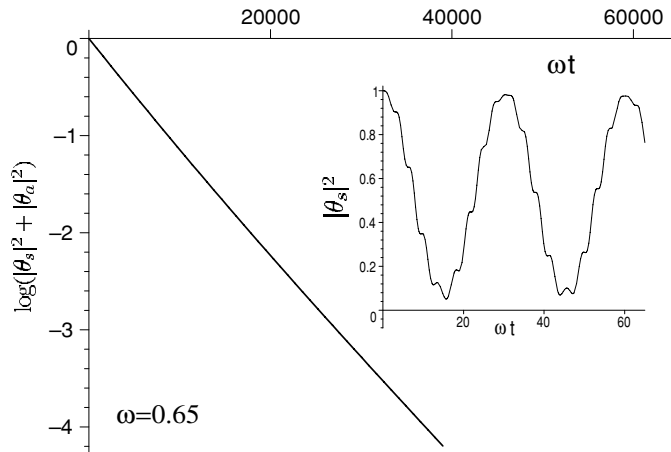
Figure 8. Plot of $\log(|\theta_s(t)|^2 + |\theta_a(t)|^2)$ for the 2-photon ionization when $\omega_a = \omega_s/2$. The initial stage of $|\theta_s(t)|^2$ dynamics is shown in the inset.
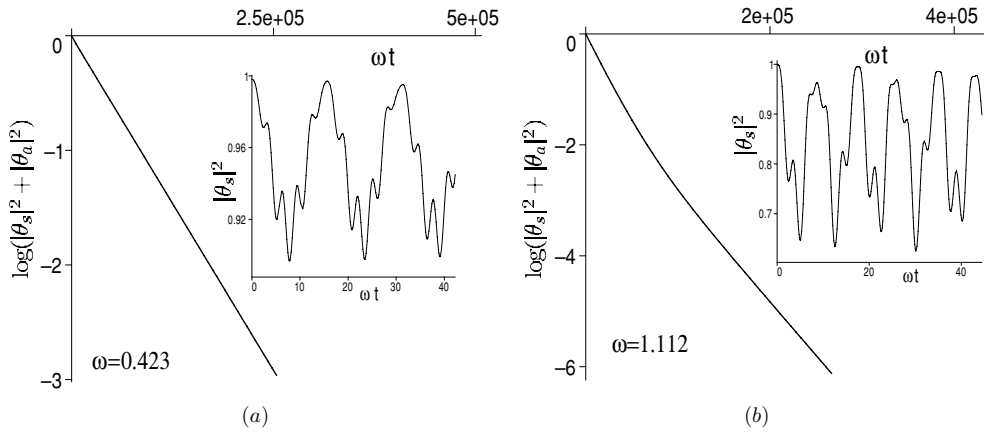

Figure 9. (a) Decay process for $\omega_a = \omega_s/4$, (b) decay process for $\omega_a = 0.75\omega_s$.

our result onto reality the unusual process above would remain almost unaffected because for example in the visible region we have $\omega T \sim (4..7) \times 10^7$ while in figure 7(b) the inversion occurs much earlier: $|\theta_a(t)|^2| \gg \theta_s(t)|^2$ when $\omega t \sim 3 \times 10^3$. We think that in a real system this type of the population inversion can also be observed because only a slower decay of the excited state compared with the ground one is required. Though it does not promise a practically acceptable efficiency, the lasing medium for the frequency $\omega_s - \omega_a$ can occur in a natural environment near a strong source of radiation, say in the stellar atmospheres.

In figures 8 and 9 we show how the location of the excited level influences the 2-photon ionization by using the cases (i), (ii) and (iii) with different ω_s, ω_a introduced earlier for $r = 0.1$ and $\omega \approx 0.545\omega_s$ for all cases. In the insets are plotted $|\theta_s(t)|^2$ for short times to show the amplitudes of the inter-level transitions.

One can see in figure 8 that the particle jumps between the bound states, but the total survival probability decays smoothly; the exponents Re ν_s are Re ν_a might be different, but this does not matter because the faster process in this case determines the rate of decay
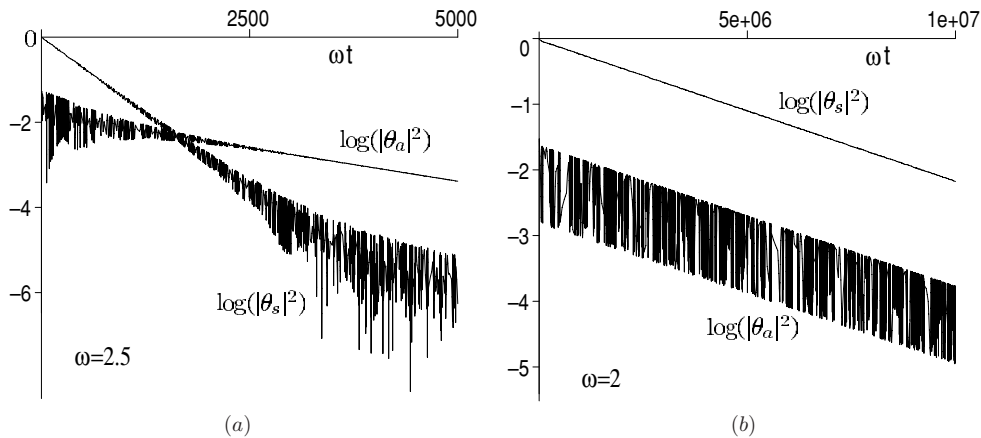
Figure 10. (*a*) Plots of $\log(|\theta(t)|^2)$ for $\omega > \omega_s$, (*b*) plots of $\log(|\theta(t)|^2)$ for $\omega_a < \omega < \omega_s$.

since the particle spends almost the same time in each level. Transitions between the energy levels are less effective in figure 9 where $\log(|\theta_s(t)|^2 + |\theta_a(t)|^2)$ are shown and the frequency of perturbation ω is farther from both frequencies ω_a and $\omega_s - \omega_a$. The decay is slower in both cases compared with figure 8, but in the case (ii) it goes mainly from the ground state where $-\mathrm{Re}\,\nu_s = 5.67 \times 10^{-6} \ll -\mathrm{Re}\,\nu_a$. For $\omega_a = 0.75\omega_s$ in figure 9(*a*), where $-\mathrm{Re}\,\nu_s = 3.53 \times 10^{-5}$, $-\mathrm{Re}\,\nu_a = 1.97 \times 10^{-5}$, the decay eventually goes mainly from the excited level: it is faster initially when the ground state is still populated. The insets in figure 9 show $|\theta_s|^2$ on the initial stage of decay. The excited level has about 5% of the ground level population in the case (ii) and 20–25% in the case (iii). The decay in the form of two exponents is more visible when the inter-level transitions are not strong (compare figure 9(*b*) with figure 8). Though the non-exponential decay is a natural process at later times, in the case of ω very close to a Stark shifted energy of a bound state even one-level systems exhibit this property much earlier [3], and such a decay was observed experimentally in unstable systems even without perturbation [14].

Now we increase the frequency of perturbation in the case (iii). The inversion of population is possible when both levels need two photons for the ionization, but this inversion is especially spectacular for the one-photon process in figure 10(*a*) when $\omega \approx 1.2\omega_s \approx 1.6\omega_a$ and $\nu_a \approx \nu_s/5$. For $\omega = 0.98\omega_s = 1.31\omega_a$ the ionization of the ground state requires two photons and thus $\nu_a \approx 50\nu_s$; therefore we observe in figure 10(*b*) a more usual dynamics: the slowly decaying ground state feeds the excited one and their very different populations are falling with same rate. Note that violent oscillations of a low populated level correspond to shallow invisible ripples on the graph of much more populated one.

A simple analysis of (24) or (A.7) shows that the main frequency which determines 'periodicity' of the transitions between the bound states can be ω and $|\Delta - \omega|$ on different stages of the decay. If ω is very large both these frequencies are close or equal to ω that we observed for $\omega = 10$, $\omega_s = 1.2$. Otherwise the level populations oscillate with the frequency which can be very different from ω as is seen in the insets of figures 8 and 9. In a special case of $|\omega - \Delta| < r^2$ on a short time interval, $tr < 1$, equations (24) yield in the first order in r

$$\theta_s(t) \approx \theta_s(0) - r\alpha\beta\theta_a(0)t, \qquad \theta_a(t) \approx \theta_a(0) + r\alpha\beta\theta_s(0)t. \qquad (29)$$

This presents a signature of the Rabi oscillations [16] of the populations $|\theta_s(t)|^2$, $|\theta_a(t)|^2$ in the form $\theta_s(t) = \theta_s(0)\cos\Omega t - \theta_a(0)\sin\Omega t$, $\theta_a(t) = \theta_a(0)\cos\Omega t + \theta_s(0)\sin\Omega t$ with the

frequency $\Omega = 2r\alpha\beta$ which is equal to the matrix element $\langle u_s|V_1|u_a\rangle$ for the transitions between the bound states. These oscillations do not develop later because they require a better tuning than $|\omega - \Delta_s|, |\omega - \Delta_a| \sim r^2$, see (25), which we have in the presence of transitions to continuum. We expect that in the case of a multiphoton ionization, the imaginary part of detuning can be very small and the Rabi beets might dominate the initial stage of evolution.

In the long run both states decay with the same rate because the slower decaying state supplies the other by the inter-level transitions, but when $\theta_{s/a}(t)$ are very small the neglected $t^{-3/2}$ term, which comes from the branch cuts, might change the whole picture. The physical origin of this term is transitions to the bound states from the continuum [5]. These transitions can be more effective for populating one of our states depending on ω. Note that though the condition of equidistance $\omega_a = \omega_s/2$ used in figure 7 does not hold in figure 10(a), the population inversion occurs readily.

6. Perturbation theory

The standard perturbation theory for transition into the continuum, which leads to the Fermi golden rule [17], can be easily implemented for our model when $\omega > \omega_s$. We iterate once in (14) to obtain $Y^\pm$ up to the order r^2. Substituting the results in (11) we have for the case $\theta_s(0) = 1, \theta_a(0) = 0$

$$\theta_s(t) = 1 - 2r^2\alpha^2 \int_0^t K_a(t')\, e^{-i\omega_s t'}[(t - t')\cos\omega t' - \omega^{-1}\sin\omega(t - t')\cos\omega t]\,dt'.$$

Using the same reasoning as in [10, 17], letting t become very large while keeping $r^2 t \ll 1$ we neglect all terms but $t\cos\omega t'$ in the square parentheses and consider the integral as the Laplace transform of $K(t)$. The result reads

$$\theta_s(t) = 1 - t\mu_s, \qquad \mu_s = r^2\alpha^2[\tilde{K}_a(i\omega_s - i\omega) + \tilde{K}_a(i\omega_s + i\omega)]. \qquad (30a)$$

Following Fermi [17] we treat (30a) as the series expansion of an exponential function $\exp(-\mu_s t)$ which is consistent with (25) (though without terms $\exp(\pm 2i\omega)$) and μ_s is equal to ν_s given in (23) to order r^2. The transitions between the bound states do not fit this scheme since for $\omega \neq \omega_s - \omega_a$ there are no long time contributions to $\theta(t)$ in the Born approximation.

In the case when in the initial state $\theta_s(0) = 0, \theta_a(0) = 1$ the same approach yields

$$\theta_a(t) \approx e^{-\mu_a t}, \qquad \mu_a = r^2\beta^2[\tilde{K}_s(i\omega_a - i\omega) + \tilde{K}_s(i\omega_a + i\omega)], \qquad (30b)$$

which is consistent with (23) to order r^2. Thus, the low order perturbation theory gives the right answer for the decay exponents and the dynamic Stark effect in the limit $r \to 0$. The full evaluation of $\theta_s(t), \theta_a(t)$ requires one more iteration in (15) and some modifications in order to avoid divergences at the resonances.

In figure 11 we plot the ratio of our results for ν and that given by the perturbation theory, equations (30a, b), Re ν/Re μ versus ω for $r = 0.3, 0.5$. The divergences between our method and the perturbation theory become significant near the Ramsauer resonances where the transition into the continuum becomes of order r^4 (the curves in fact go to ∞ because Re $\mu = 0$ there). Though we study only moderate r our results can be expected to stay reliable up to $r \sim 0.7$.

The ratios Re ν/Re μ as functions of r for two frequencies $\omega = 1.22$ and $\omega = 1.3$ are shown in figures 12 and 13 for the case $\omega_s \approx 2\omega_a$.

Though $\omega_s \approx 1.19$ a 'photon' with energy 1.22 can ionize the system via the one-photon process only when $r < 0.25$. For larger r the Stark effect shifts the ground level down and for its ionization two such photons are needed. This is not captured by the perturbation theory
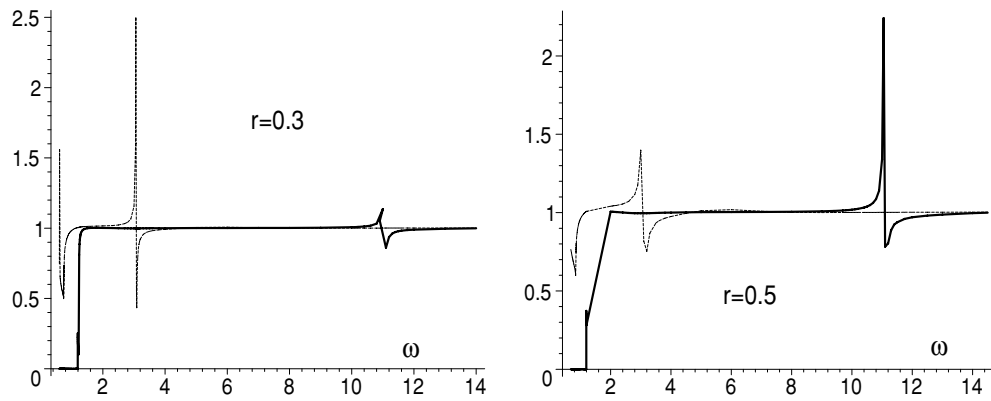
Figure 11. Plots of $\mathrm{Re}\,\nu_s/\mathrm{Re}\,\mu_s$ (solid line) and $\mathrm{Re}\,\nu_a/\mathrm{Re}\,\mu_a$ (dotted line) versus ω for $q \approx 2$, $\omega_s \approx 1.19 \approx 2\omega_a$.
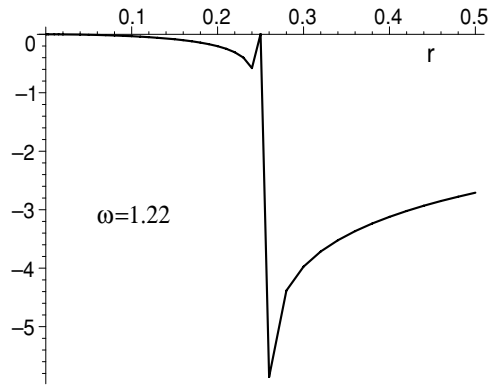
Figure 12. Plot of $\log(\mathrm{Re}\,\nu_s/\mathrm{Re}\,\mu_s)$ versus r for $\omega = 1.22$.
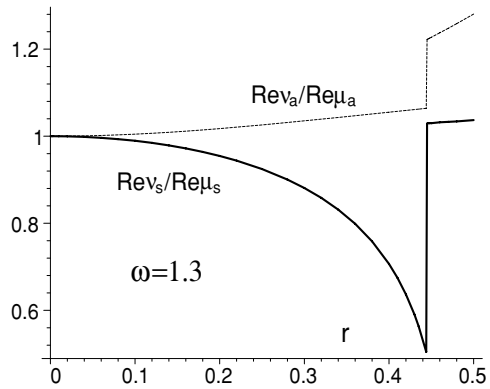

Figure 13. Plots of $(\mathrm{Re}\,\nu/\mathrm{Re}\,\mu)$ versus r for $\omega = 1.3$.

which fails noticeably for $r > 0.18$. When $\omega = 1.3$ this effect is clearly weaker: the one-photon ionization persists for $r = 0.5$, but the perturbation result is two times larger than $\mathrm{Re}\,\nu_s$

for $r = 0.44$. The ionization of the excited level goes always here via the one-photon process but, as is seen in figure 13, it varies noticeably when r increases, though the perturbation theory does not describe this.

All in all the lowest order perturbation theory gives good results for the rate of decay up to $r = 0.5$ as long as ω is not near a resonance, see also [18].

7. Discussion and implications for real systems

This work was motivated partially by the following question: does the position of the excited level strongly influence the ionization process. Our findings are that the results are different for one- and two-photon ionization.

(a) The one-photon ionization rate for $\omega > \omega_s$ is, in non-resonance conditions, only weakly affected by the position of the excited state and by the initial populations of the different levels (figures 2–4). After a relatively short time of redistribution almost all the remaining bound population stays in one of the bound states (figures 7 and 10).

(b) In the two-photon ionization, when the frequency of the perturbation is approximately 10% higher than one-half of the binding energy of the ground state ω_s, the position of the excited level can be important. When ω_a/ω_s is 1/4, 3/4 the rate of decay is about 10 and 4 times respectively lower than in the case $\omega_a/\omega_s = 0.5$. The population oscillates between the two levels almost from 0 to 1 for $\omega_a/\omega_s = 0.5$, but less than 10% for $\omega_a/\omega_s = 1/4$ and about 25% for $\omega_a/\omega_s = 3/4$. In the latter case the decay process differs distinctly from exponential if the particle starts in the ground level because the excited level decays slower. When the frequency of the perturbation is very close to the energy difference between the bound states their populations, in the initial stage of the decay, oscillate with the Rabi frequency.

The behaviour of the energy level dynamics found here should be observable experimentally in a real system with only two discrete states (plus the continuum) or if these two states are distinctly separated from all others which are close to the continuum. It is also preferable to study relatively low energy atomic and molecular levels where transitions only slightly affect the effective potential field so one-particle electronic states give a good approximation.

(c) The inverse Ramsauer effect makes the decay rate in our model very small at the resonance frequencies (see figures 2–4) which are different for the two levels. If the inter-level transitions are low (this should be studied using (A.7) for our model) one might expect a so-called stabilization at these resonances.

The noble gases, especially the light ones Ar, Xe, Kr, demonstrate a very strong Ramsauer effect in collisions with electrons at the energies 0.6–0.9 eV [20]. Some simple molecules, say methane CH_4 also have this property. This suggests an experimental check on the photoionization of these gases by long laser pulses at the corresponding frequencies. For argon this effect should be expected at wavelengths 75–77 nm, for xenon at 99–101 nm and for krypton at 77–82 nm, i.e. about 0.5–1 eV above the ionization threshold. There is a possibility of observing the same effect in experiments with molecular photodetachment [20].

We do not study here short pulse processes which are also sensitive to the shape of pulses.

8. Conclusion

Our model is probably the simplest example (compare, say with [19]) of a system in which one can explicitly see the interplay between transitions among bound states and the continuum, i.e.

ionization, caused by an external periodic excitation. It extends previous studies by us [3–5] and by other authors [2] of a model with only one bound state, where $V_0(x) = -q\delta(x)$. The simplicity of our model allows the use of a non-perturbative analysis of its time evolution. This brings out certain phenomena which we expect to also hold for real systems. We chose the parameters of the unperturbed system as well as the frequency and amplitude of the external forcing so that we could construct an approximate analytical solution for the cases of one- and two-photon ionization and study details of the process in different regimes. The multiphoton ionization can also be treated by our approximate scheme due to its convergence.

Comparing our results with the standard first-order perturbation theory we find that even when the latter gives a good approximation to the ionization rate for $\hbar\omega$ large compared to the binding energy, it fails (as expected) to take into proper account the role of the excited level in the ionization. This becomes very important when ω or its multiples are close to resonances, e.g. to ω_s, ω_a, or $\Delta = \omega_s - \omega_a$.

Acknowledgments

Appendix

A.1. Main details of the computation

Accepting (22) and moderate r we need only $\tilde{Y}_n^{\pm}(p)$ with $0 \leqslant n \leqslant 3$ and $0 \leqslant \operatorname{Im} p < \omega$ for integration in (19). The integration is reduced to the evaluation of residues and due to the fact that $e^{pt}/p \neq 0$ at all poles of $\tilde{Y}$ we compute the residues $\operatorname{Res}\{\tilde{Y}_n^{\pm}(p)\} = X_n^{\pm}$. Obviously these quantities are the solutions of two homogeneous recurrence relations associated with (21)

$$c_k^- X_k^- = r^2\left(a_{k+2}s_{k+1}X_{k+2}^- + a_{k-2}s_{k-1}X_{k-2}^-\right), \qquad c_k^+ X_k^+ = r^2\left(s_{k+2}a_{k+1}X_{k+2}^+ + s_{k-2}a_{k-1}X_{k-2}^+\right),$$
(A.1)

where $-\infty < k < \infty$. The condition for convergence

$$X_k^{\pm} \to 0, \qquad \text{when} \quad |k| \to \infty$$

gives the location of poles of $\tilde{Y}_k^{\pm}$ (Fredholm's alternative). The two recurrences in (A.1) are formally identical: f^-, g^- play the same role for $X^-(p)$, $\tilde{Y}^-(p)$ as f^+, g^+ for $X^+(p)$, $\tilde{Y}^+(p)$. Introducing new variables $\rho_k^{\pm}(p) = c_{2k+2}^{\pm}X_{2k+2}^{\pm}/c_{2k}^{\pm}X_{2k}^{\pm}$ we represent (A.1) as

$$\rho_n^{\pm} = \frac{1}{f_{n+1}^{\pm}}\left(\frac{1}{r^2} - \frac{g_{n-1}^{\pm}}{\rho_{n-1}^{\pm}}\right), \qquad n \in Z.$$
(A.2)

Using the continuous fraction representation for ρ_0 in both directions and equating them after the truncation we obtain equations for the location of the initial poles

$$\begin{aligned}
r^4\left(f_1^- g_0^- + f_0^- g_{-1}^-\right) &= 1 & \text{at} \quad p = i\omega_a + \nu_a; \\
r^4\left(f_1^+ g_0^+ + f_0^+ g_{-1}^+\right) &= 1 & \text{at} \quad p = i\omega_s + \nu_s,
\end{aligned}$$
(A.3)

where we neglected terms which give corrections of order r^6 and higher. Equations (A.3) imply (23) immediately. One can evaluate approximately

$$X_{-2}^{\pm} = \frac{c_0^{\pm}X^p m_0}{\rho_{-1}^{\pm}c_{-2}^{\pm}}, \qquad X_2^{\pm} = \frac{c_0^{\pm}\rho_0^{\pm}X_0^{\pm}}{c_2^{\pm}}$$
(A.4)

in terms of $X_0^\pm$ as soon as ρ_0 and ρ_{-1} are computed by (A.2):

$$\rho_0 = \frac{1}{f_1}\left(\frac{1}{r^2} - \frac{r^2 g_{-1} f_0}{1 - r^4 g_{-2} f_{-1}}\right) = \frac{g_0 r^2}{1 - r^4 f_2 g_1}, \qquad \rho_{-1} \approx \frac{r^2 g_{-1}}{1 - r^2 f_1 \rho_0},$$

where we dropped superscripts. This scheme, constructed here for the one- and two-photon ionization, can be easily generalized. It allows us to use straightforward computations in (21) only near the points $i\omega_s$, $i\omega_a$, $i\omega_s - i\omega$, and $i\omega_a - i\omega$ and then cover the interval from $i\omega_a - 3i\omega$ to $i\omega_s + 3i\omega$ with the help of functions ρ_0, ρ_{-1}. Thus, we neglect all virtual processes involving more than three photons.

In this spirit one can make only two iterations up and down in the recurrences (21) starting at $k = 0$ and obtain their approximate solutions

$$\tilde{Y}_0^\pm \equiv \tilde{Y}^\pm(p) = r\frac{b_0^\pm + r^2\left(f_1^\pm b_2^\pm + g_{-1}^\pm b_{-2}^\pm\right)}{c_0^\pm\left[1 - r^4\left(f_0^\pm g_{-1}^\pm + g_0^\pm f_1^\pm\right)\right]}. \tag{A.5}$$

The functions $\tilde{Y}^\pm(p)$ here are analytical in the open right half plane. In the left half plane there are a number of poles and the horizontal cuts $p = in\omega$, $n = 0, \pm 1, \pm 2, \pm 3$, which are actually only a part of the two infinite sets involving all integers for the exact solution (see figure 1). Using (18) and (A.5) one can see that

$$\tilde{Y}^-(i\lambda^2) = -i\frac{\theta_a^0}{2\beta}, \qquad \tilde{Y}^+(i\gamma^2) = -i\frac{\theta_s^0}{2\alpha},$$

and therefore from (19) we have in this approximation

$$\theta_s(\infty) = \theta_a(\infty) = 0. \tag{A.6}$$

The complete ionization for all values of r and ω is presented by equation (A.6) which is in fact generically correct in all orders, i.e. $n \to \infty$. This can be proven by methods similar to those in [5]. We do not explore here the possibility [4, 5] that (A.6) does not hold for exceptional sets of parameters.

For computing the residues of (A.5) we analyse and simplify it using (20) by neglecting terms of order r^6 and in the numerators sometimes even r^4 if they are multiplied by factors of order 1. The crucial role is played by the structure of $\tilde{K}_s(p)$ and $\tilde{K}_a(p)$. Though these functions have an infinite number of poles only the poles at $p = i\gamma^2$ and $p = i\lambda^2$ will contribute in (19). Near these poles we have respectively

$$s_0 = \tilde{K}_s(i\gamma^2 + \epsilon) = \frac{\alpha^2}{\epsilon} - if_s + O(\epsilon), \qquad f_s = \frac{1 + (q - 2\gamma)(1 + 2\gamma - 2q)}{4(1 + 2\gamma - q)^2},$$

$$a_0 = \tilde{K}_a(i\lambda^2 + \epsilon) = \frac{\beta^2}{\epsilon} - if_a + O(\epsilon), \qquad f_a = \frac{1 + (q - 2\lambda)(1 + 2\lambda - 2q)}{4(1 + 2\lambda - q)^2}.$$

The functions $S_{\pm 1}$, $A_{\pm 1}$ are singular at these points too:

$$S_{\pm 1}(i\gamma^2 + \epsilon) = \alpha\theta_s^0\left(\mp\frac{i}{2\epsilon} + \frac{1}{4\omega}\right) + O(\epsilon), \qquad A_{\pm 1}(i\lambda^2 + \epsilon) = \beta\theta_a^0\left(\mp\frac{i}{2\epsilon} + \frac{1}{4\omega}\right) + O(\epsilon).$$

A careful but straightforward computation of $\text{Res}\{\tilde{Y}_j^{\pm}\}$ on the interval $[0, \omega]$ with $j = 0, 1, -1$ and using (A.3) yields eventually θ_s, θ_a in the form

$$
\begin{aligned}
\theta_s(t) &= e^{\nu_s t}\left(1 + \frac{i\nu_s}{2\omega}\frac{a_1 e^{2i\omega t} - a_{-1} e^{-2i\omega t}}{a_1 + a_{-1}}\right)\frac{R_2}{U_2} \\
&\quad + ir\alpha\beta\, e^{-i\Delta_a t}\left[\left(\frac{e^{i\omega t}}{\omega - \Delta_a} + r^2 s_1 a_2\frac{e^{3i\omega t}}{3\omega - \Delta_a}\right)\frac{R_3}{U_3}\right. \\
&\quad\quad \left. + \left(\frac{e^{-i\omega t}}{\omega + \Delta_a} + r^2 s_{-1}a_{-2}\frac{e^{-3i\omega t}}{3\omega + \Delta_a}\right)\frac{R_5}{U_3}\right], \\
\theta_a(t) &= e^{\nu_a t}\left(1 + \frac{i\nu_a}{2\omega}\frac{s_1 e^{2i\omega t} - s_{-1} e^{-2i\omega t}}{s_1 + s_{-1}}\right)\frac{R_1}{U_1} + ir\alpha\beta\, e^{i\Delta_s t}\left[\left(\frac{e^{-i\omega t}}{\omega - \Delta_s} + r^2 a_1 s_2\frac{e^{3i\omega t}}{3\omega + \Delta_s}\right)\frac{R_4}{U_4}\right. \\
&\quad \left. + \left(\frac{e^{-i\omega t}}{\omega + \Delta_a} + r^2 a_{-1}s_{-2}\frac{e^{-3i\omega t}}{3\omega - \Delta_s}\right)\frac{R_6}{U_4}\right].
\end{aligned}
$$

$$\text{(A.7)}$$

Here we use the notations

$$
\begin{aligned}
R_1 &= -r^2\beta^2\theta_a^0\left[\frac{s_1 + s_{-1} + r^2 s_1 s_{-1}(a_2 + a_{-2})}{\nu_a} + i\frac{s_1 - s_{-1}}{2\omega}\right] \\
&\quad - 2ir\alpha\beta\omega\theta_s^0\left[\frac{1 + r^2 a_{-2}s_{-1}}{\omega^2 - \Delta_a^2} + \frac{2r^2 a_2 s_1}{(\omega + \Delta_a)(3\omega - \Delta_a)}\right], \\
R_2 &= -r^2\alpha\theta_s^0\left[\frac{a_1 + a_{-1} + r^2 a_1 a_{-1}(s_2 + s_{-2})}{\nu_s} + i\frac{a_1 - a_{-1}}{2\omega}\right] \\
&\quad - 2ir\alpha\beta\omega\theta_a^0\left[\frac{1 + r^2 s_2 a_1}{\omega^2 - \Delta_s^2} + \frac{2r^2 s_{-2}a_{-1}}{(\omega + \Delta_s)(3\omega - \Delta_s)}\right], \\
R_3 &= \theta_a^0\left[1 + \frac{i\nu_a}{2\omega} + r^2 s_{-1}\left(a_{-2} + \frac{i\beta^2}{\omega}\right)\right] \\
&\quad - 2ir\alpha\beta\omega\theta_s^0\left[\frac{1 - i\nu_a f_a\beta^{-2} + r^2 s_{-1}a_{-2}}{\omega^2 - \Delta_a^2} - a_2\frac{r^2 s_{-1} + \nu_a\beta^{-2}}{\omega^2 - (2\omega - \Delta_a)^2}\right], \\
R_4 &= \theta_s^0\left[1 + \frac{i\nu_s}{2\omega} + r^2 a_{-1}\left(s_{-2} + \frac{i\alpha^2}{\omega}\right)\right] \\
&\quad - 2ir\alpha\beta\omega\theta_a^0\left[\frac{1 - i\nu_s f_s\alpha^{-2}}{\omega^2 - \Delta_s^2} + \frac{2r^2 s_{-2}a_{-1}}{(\omega + \Delta_s)(3\omega - \Delta_s)}\right], \\
R_5 &= \theta_a^0\left[1 - \frac{i\nu_a}{2\omega} + r^2 s_1\left(a_2 - \frac{i\beta^2}{\omega}\right)\right] \\
&\quad - 2ir\alpha\beta\omega\theta_s^0\left[\frac{1 - i\nu_a f_a\beta^{-2}}{\omega^2 - \Delta_a^2} + \frac{2r^2 a_2 s_1}{(\omega + \Delta_a)(3\omega - \Delta_a)}\right], \\
R_6 &= \theta_s^0\left[1 - \frac{i\nu_s}{2\omega} + r^2 a_1\left(s_2 - \frac{i\alpha^2}{\omega}\right)\right] \\
&\quad - 2ir\alpha\beta\omega\theta_a^0\left[\frac{1 - i\nu_s f_s\alpha^{-2} + r^2 a_1 s_2}{\omega^2 - \Delta_s^2} - s_{-2}\frac{r^2 a_1 + \nu_s\alpha^{-2}}{\omega^2 - (2\omega - \Delta_s)^2}\right].
\end{aligned}
$$

The functions U_n involve the derivatives of $a(p), s(p)$

$$U_1 = 1 + r^2[\beta^2(s_1' + s_{-1}') + (a_2 - if_a)(s_1 + v_a s_1') + (a_{-2} - if_a)(s_{-1} + v_a s_{-1}')],$$

$$U_2 = 1 + r^2[\alpha^2(a_1' + a_{-1}') + (s_2 - if_s)(a_1 + v_s a_1')) + (s_{-2} - if_s)(a_{-1} + v_s a_{-1}')],$$

$$U_3 = U_1 + r^4\beta^2(a_2 + a_{-2})(s_1's_{-1} + s_1 s_{-1}'), \qquad U_4 = U_2 + r^4\alpha^2(s_2 + s_{-2})(a_1'a_{-1} + a_1 a_{-1}').$$

All the functions s_k, a_n which define $\theta(t)$ here should be evaluated at p_a if k is odd and n is even, but at p_s if k is even and n is odd.

The truncation procedure for solving the recurrence (21) can be implemented effectively for the multiphoton ionization too when r is small using the following technique. Let $|\omega_s/\omega - N| < 1, |\omega_a/\omega - M| < 1$ for some positive integers N, M. It is easy for an approximate calculation to figure out which functions s_n, a_m can be large on the interval $0 \leqslant \operatorname{Im} p < \omega$ and iterate one or two steps (depending on r) up and down near N and M neglecting corresponding $\tilde{Y}_k^\pm$. This will allow us to construct a close algebraic set from (21). We leave details of this approach for the future.

A.2. Poles of functions $\tilde{K}_{s/a}$.

The Laplace transforms of functions $K_{s/a}(t)$ (15) can be written in the form

$$\tilde{K}_s(p) = \frac{\alpha^2}{p - i\gamma^2} + \frac{q}{\pi} \int_0^\infty \frac{dk}{(p + ik^2)[1 + (\tan k + q/k)^2]},$$

$$\tilde{K}_a(p) = \frac{\beta^2}{p - i\lambda^2} + \frac{q}{\pi} \int_0^\infty \frac{dk}{(p + ik^2)[1 + (\cot k - q/k)^2]}. \tag{A.8}$$

For the contour integration in (A.8) one needs to know the location of poles in the integrands. The relation $1 + (\tan k + q/k)^2 = 0$ is equivalent to a pair of equations

$$1 + e^{2ik} + \frac{2ik}{q} = 0, \qquad 1 + e^{-2ik} - \frac{2ik}{q} = 0, \tag{A.9}$$

whose solutions differ in sign. Defining temporarily for convenience new quantities $q + 2ik = \rho_s \exp(i\varphi_s)$ we rewrite one of the equations (A.9) as

$$\rho_s \sin \varphi_s = (2n - 1)\pi + \varphi_s, \qquad \rho_s \cos \varphi_s = q - \ln q + \ln \rho_s, \tag{A.10}$$

where $n \in Z$ and $0 < \varphi_s < \pi$ if $n \geqslant 1, \pi < \varphi_s < 2\pi$ if $n \leqslant -1, \varphi_s = \pi$, when $n = 0$. The case $n = 0, \varphi_s = \pi$ yields the solution corresponding to the bound state $k = i\gamma$, for each other n (A.10) has a single solution k_n with $\operatorname{Im}(k_n) < 0$ and the following asymptotics

$$\operatorname{Re}(k) \to n\pi, \qquad \operatorname{Im}(k) \to -\ln|n|. \tag{A.11}$$

The equation $1 + (\cot k - q/k)^2 = 0$, after its reduction to $e^{2ik} = 1 + 2ik/q$ and using the notation $q + 2ik = \rho_a \exp(i\varphi_a)$, gives

$$\rho_a \sin \varphi_a = 2n\pi + \varphi_a, \qquad \rho_a \cos \varphi_a = q - \ln q + \ln \rho_a, \tag{A.12}$$

where $0 < \varphi_a < \pi$ if $n \geqslant 1$ and $\pi < \varphi_a < 2\pi$ if $n \leqslant -1$. For $n = 0$ we get $\varphi_a = 0$ and $k = i\lambda$. When $n \neq 0$ equation (A.12) for each n produces a single root in the lower half plane with the asymptotics (A.11). These solutions should be supplemented with a similar set having the opposite sign. Let us consider for example the first of the integral terms in (A.8). We rewrite it as

$$\frac{q}{2\pi} \int_{-\infty}^\infty \frac{dk}{(p + ik^2)(\tan k + i + q/k)(\tan k - i + q/k)}$$

and transform it into the form

$$\frac{q\mathrm{i}}{2\pi} \int_{-\infty}^{\infty} \frac{k(\mathrm{e}^{2ik} + 1)\,\mathrm{d}k}{(p + ik^2)[2ik + q(\mathrm{e}^{2ik} + 1)]},$$

which permits us to close the contour of integration over the upper half plane. The crucial point is the presence of only two poles of the integrand inside the contour: at $k = \sqrt{ip}$ and $k = i\gamma$ because the infinite set of other poles is located in the lower half plane. A simple evaluation of residues yields (18a). For the (18b) the technique is similar, but the second pole occurs at $k = i\lambda$ when $q > 1$. It is absent for $q < 1$.

References

[1] Pindzola M S and Dörr M 1991 *Phys. Rev.* A **43** 439
Buchleitner A, Delande D, Zakrzewski J, Mantegna R N, Arndt M and Walther H 1995 *Phys. Rev. Lett.* **75** 3818
Pan L, Taylor K T and Clark C W 1991 *Phys. Rev.* A **43** 6272
Volkova E A, Popov A M and Tikhonova O V 1998 *JETP* **86** 71
[2] Geltman S 1977 *J. Phys. B: At. Mol. Phys.* **10** 831
Scharf G, Sonnenmoser K and Wreszinski W F 1991 *Phys. Rev.* A **44** 3250
[3] Rokhlenko A, Costin O and Lebowitz J L 2002 *J. Phys. A: Math. Gen.* **35** 8943
Costin O, Costin R D, Lebowitz J L and Rokhlenko A 2001 *C. R. Acad. Sci. Paris* **332** 405
Costin O, Costin R D, Lebowitz J L and Rokhlenko A 2001 *Commun. Math. Phys.* **221** 1
[4] Costin O, Lebowitz J L and Rokhlenko A 2001 Mathématiques Centre de Recherches *CRM Proc. Lect. Notes* **27** 51
Costin O, Costin R D and Lebowitz J L 2004 *J. Stat. Phys.* **116** 311
[5] Costin O, Lebowitz J L and Rokhlenko A 2000 *J. Phys. A: Math. Gen.* **33** 6311
[6] Garcia-Calderon G, Mateos J L and Moshinsky M 1995 *Phys. Rev. Lett.* **74** 337
Soffer A and Weinstein M I 1998 *J. Stat. Phys.* **93** 359
[7] Becker W, Kundrotas J and Dargys A 1986 *Phys. Status Solidi* B **134** 267
McIver J K and Confer 1989 *Phys. Rev.* A **40** 6904
Susskind S M, Cowley S C and Valeo E J 1990 *Phys. Rev.* A **42** 3090
[8] Dörr M, Latinne O and Joachain C J 1997 *Phys. Rev.* A **55** 3697
Bardsley J N and Comella M J 1989 *Phys. Rev.* A **39** 2252
[9] Koch P M and van Leeuwen K A H 1995 *Phys. Rep.* **255** 289
Koch P M 1998 *Acta Phys. Pol.* A **93** 105
[10] Landau L D and Lifschitz E M 1965 *Quantum Mechanics—Nonrelativistic Theory* 2nd edn (New York: Pergamon)
[11] Schiff L I 1955 *Quantum Mechanics* 2nd edn (New York: McGraw-Hill)
[12] Cohen-Tannoudji C, Duport-Roc J and Arynberg G 1992 *Atom-Photon Interactions* (New York: Wiley)
[13] Maquet A, Chu Shih-I and Reinhardt W P 1983 *Phys. Rev.* A **27** 2946
Autler S H and Townes C H 1955 *Phys. Rev.* **100** 703
[14] Heitler W 1954 *The Quantum Theory of Radiation* 3rd edn (New York: Oxford)
[15] Wilkinson S R *et al* 1997 *Nature* **387** 575
[16] Rabi I I 1937 *Phys. Rev.* **51** 652
Scully M O and Zubairy M S 1997 *The Quantum Optics* (Cambridge: Cambridge University Press)
[17] Fermi E 1961 *Notes on Quantum Mechanics* (Chicago: The University of Chicago Press)
[18] Potvliege R M and Shakeshaft R 1989 *Phys. Rev.* A **40** 3061
[19] Shirley J H 1965 *Phys. Rev.* B **138** 979
[20] Massey H S W, Burhop E H S and Gilbody H B 1969 *Electronic and Ionic Impact Phenomena* 2nd edn (Oxford: Clarendon)
Brown S C 1994 *Basic Data of Plasma Physics* (New York: AIP)